



Biocompatibility of core@shell particles: Cytotoxicity and genotoxicity in human osteosarcoma cells of colloidal silica spheres coated with crystalline or amorphous zirconia

A.L. Di Virgilio ^{a,b,*}, P.M. Arnal ^c, I. Maisuls ^{b,c}^a CEQUINOR (*Centro de Química Inorgánica*), Facultad de Ciencias Exactas, UNLP, 47 y 115 (1900), La Plata, Argentina^b Cátedra de Bioquímica Patológica, Facultad de Ciencias Exactas, UNLP, 47 y 115 (1900), La Plata, Argentina^c CETMIC (*Centro de Tecnología de Recursos Minerales y Cerámica*), Cno Centenario y 506, CC 49 (B1897ZCA), M.B. Gonnet, Prov. Buenos Aires, Argentina

ARTICLE INFO

Article history:

Received 13 March 2014

Received in revised form 5 May 2014

Accepted 26 May 2014

Available online 6 June 2014

Keywords:

Core@shell materials

Cytotoxicity

Genotoxicity

Zirconia

Silica

Human osteosarcoma cells

ABSTRACT

The cytotoxicity and genotoxicity of novel colloidal silica spheres coated with crystalline or amorphous zirconia ($\text{SiO}_2@\text{ZrO}_2^{\text{cryst}}$ or $\text{SiO}_2@\text{ZrO}_2^{\text{am}}$) have been studied in a human osteosarcoma cell line (MG-63), after 24 h exposure. $\text{SiO}_2@\text{ZrO}_2^{\text{cryst}}$ and $\text{SiO}_2@\text{ZrO}_2^{\text{am}}$ had mean diameters of 782 ± 19 and 891 ± 34 nm, respectively. $\text{SiO}_2@\text{ZrO}_2^{\text{cryst}}$ exposure reduced cell viability, with an increase in reactive oxygen species (ROS) and a decrease of the GSH/GSSG ratio. The comet and micronucleus (MN) assays detected DNA damage at 5 and 25 $\mu\text{g}/\text{mL}$, respectively. $\text{SiO}_2@\text{ZrO}_2^{\text{am}}$ induced genotoxic action only at 10 and 50 $\mu\text{g}/\text{mL}$ (comet and MN assays), along with a decrease of the GSH/GSSG ratio at 50 $\mu\text{g}/\text{mL}$. Both particles were found inside the cells, forming vesicles; however, none of them entered the nucleus. Our findings show that crystallization of the shell of the amorphous ZrO_2 increases both cytotoxicity and genotoxicity.

© 2014 Elsevier B.V. All rights reserved.

1. Introduction

Core@shell particles are nano or micro-sized particles which have a core and a shell of different structure/composition, as opposed to conventional nanoparticles, which have a homogenous structure [1]. They are classified broadly based on the material with which the core and shell are made. Recently, core@shell nanoparticles have found widespread applications as catalysts, modifiers, fillers, and thermal/mechanical property enhancers. Biomedical applications include imaging, drug delivery, and use as intracellular biomarkers [2–4]. Particles of metal oxides are used in optical bioimaging and in fluorescence and magnetic imaging [5–8].

Regarding the toxicity of such particles, several reports note injurious effects of nanoparticles in cell lines – cytotoxicity, oxidative stress, and inflammatory responses [9–12]. Studies on the genotoxicity of metal oxide particles have reported micronucleus (MN) induction [13,14], DNA damage detected by the comet assay [15], and chromosomal aberrations [16]. However, there are

contrary reports. Theogaraj et al. [17] and Warheit et al. [18] did not find TiO_2 nanoparticles to be genotoxic: they did not observe DNA damage in the chromosomal aberration test in Chinese hamster ovary (CHO) cells. Information on the toxicity of colloidal core@shell particles is scarce. They have been evaluated in some *in vitro* biological systems, indicating that biocompatibility has to be evaluated on a case-by-case basis.

Zirconia-based ceramics are routinely used in structural applications in engineering, such as in the manufacture of cutting tools, gas sensors, refractories and structural opacifiers, and in medical and dental care [19]. In dentistry, zirconia has been used for making crowns, bridges, abutments, and implant prostheses infrastructures [20]. *In vitro* and *in vivo* studies confirmed a high biocompatibility of zirconia [21,22] which is a chemically inert material and allows good cell adhesion; no adverse systemic reactions have been associated with its use [23]. Cytotoxicity, carcinogenicity, mutagenicity, or chromosomal alterations in fibroblasts or blood cells have not been observed [24]. However, particles can be released from the degradation of zirconia, promoting a localized inflammatory immune reaction [25]. Zirconia-based nanoparticles show moderate toxicity in human alveolar epithelial and macrophage cell lines [26]. Nanosized ZrO_2 showed no toxicity towards the yeast *Saccharomyces cerevisiae* [27], bacteria, algae, crustaceans, or soil bacteria [28]. We have measured possible cytotoxic and

* Corresponding author at: CEQUINOR and Cátedra de Bioquímica Patológica, Facultad de Ciencias Exactas, UNLP, 47 y 115 (1900), La Plata, Argentina.
Tel.: +54 221 4235333x49; fax: +54 221 4259485.

E-mail address: aldivirgilio@biol.unlp.edu.ar (A.L. Di Virgilio).

genotoxic effects of colloidal silica spheres coated with crystalline or amorphous zirconia ($\text{SiO}_2@\text{ZrO}_2^{\text{cryst}}$ or $\text{SiO}_2@\text{ZrO}_2^{\text{am}}$) in human osteosarcoma (MG-63) cells. To elucidate possible mechanisms of action, oxidative stress markers and cellular uptake were also measured.

2. Experimental

2.1. Materials

Tissue culture materials were purchased from Corning (Princeton, NJ, USA), Dulbecco' Modified Eagles Medium (DMEM), TrypLE™ from Gibco (Gaithersburg, MD, USA), and fetal bovine serum (FBS) from Internegocios SA (Argentina). MTT, Trypan Blue and cytochalasin B from *Dreschslera dematioidea* were purchased from Sigma Chemical Co. (St. Louis, MO, USA). Dihydrorhodamine 123 (DHR) was purchased from Molecular Probes (Eugene, OR, USA). Bleomycin (BLM) (Blocamycin®) was kindly provided by Gador S.A. (Buenos Aires, Argentina). Syber Green and low-melting-point agarose were purchased from Invitrogen Corporation (Buenos Aires, Argentina).

2.2. Methods

2.2.1. Synthesis of $\text{SiO}_2@\text{ZrO}_2^{\text{cryst}}$ and $\text{SiO}_2@\text{ZrO}_2^{\text{am}}$

We obtained both types of particles by following a previously reported procedure [29]. We checked the crystallization of the shell with X-ray diffraction (XRD) (X-ray Diffractometer, Philips PW 3020) and the shape of particles, as well as their diameter distribution, with scanning electron microscopy (SEM) (FEI Quanta 200).

2.2.2. Preparation of $\text{SiO}_2@\text{ZrO}_2$ suspensions

Fresh stock suspensions of $\text{SiO}_2@\text{ZrO}_2$ were prepared in phosphate buffered saline (PBS) at 10 mg/mL, vortexed for 10 min and stored at 4 °C in the dark. To obtain test dispersions, stock suspension was diluted with Dulbecco's Modified Eagle Medium (DMEM) at the concentrations indicated in the experiments.

2.2.3. Cell culture and incubations

The human osteosarcoma (MG-63) cell line was purchased from ATCC (CRL1427™). Cells were grown in DMEM containing 10% FBS, 100 U mL⁻¹ penicillin and 100 µg/mL streptomycin at 37 °C in a 5% CO₂ atmosphere. Cells were seeded in a 75 cm² flask and when 70–80% confluence was reached, cells were subcultured (1 mL TrypLE™ per 25 cm² flask). For experiments, cells were grown in multi-well plates. When cells reached the desired confluence, the monolayers were washed with DMEM and incubated under the conditions described below.

2.2.4. Cell viability

Cell viability was assayed by the MTT assay and by the measurement of total protein content. The MTT assay was carried out according to Mosmann [30]. Briefly, cells were treated with $\text{SiO}_2@\text{ZrO}_2^{\text{cryst}}$ or $\text{SiO}_2@\text{ZrO}_2^{\text{am}}$, 5–100 µg/mL, for 24 h. Following exposure, cells were incubated with 0.5 mg/mL MTT for 3 h. Cells were lysed in DMSO. Color development was measured at 570 nm. Results were expressed as the mean of three independent experiments and plotted as percent of control.

Total protein content measurement was performed with a commercial kit (Pierce™ BCA Protein Assay Kit) following the recommendation of manufacturers.

2.2.5. Cytokinesis-block micronucleus (MN) assay

The MN assay is used to screen potentially genotoxic compounds. MN are cytoplasmic bodies that have a portion of an

acentric chromosome or whole chromosome which was not carried during anaphase, resulting in the absence of whole chromosomes or parts of them from the main nucleus [31]. Experiments were set up with cultures in the log phase of growth. MG-63 cells were treated with $\text{SiO}_2@\text{ZrO}_2^{\text{cryst}}$ or $\text{SiO}_2@\text{ZrO}_2^{\text{am}}$ along with cytochalasin B (4.5 µg/mL). After 24 h, cells were rinsed and subjected to hypotonic conditions, fixed with methanol at -20 °C and stained with 5% Giemsa. For the analysis, 500 binucleated (BN) cells were scored at 400× magnification per experimental point from each experiment. The examination criteria employed were as reported by Fenech [32].

2.2.6. Single cell gel electrophoresis (comet assay)

For detection of DNA damage, the comet assay was employed based on the method of Singh et al. [33], with minor modifications. Briefly, MG-63 cells were treated with $\text{SiO}_2@\text{ZrO}_2^{\text{cryst}}$ or $\text{SiO}_2@\text{ZrO}_2^{\text{am}}$. After 24 h, cells were suspended in 0.5% low-melting-point agarose and immediately poured onto microscope slides precoated with 0.5% normal-melting-point agarose. Slides were immersed in ice-cold lysis solution (pH 10) for 1 h. Electrophoresis was performed at 0.8 V/cm (25 V, distance to electrodes 29.5 cm) in alkaline buffer (pH 12.7). Afterwards, slides were neutralized and stained with SyberGreen. Analysis was performed in an Olympus BX50 fluorescence microscope. Randomly captured cells, 100 per experimental point, were used to determine the tail moment, using Comet Score version 1.5 software.

2.2.7. Determination of reactive oxygen species (ROS) level

Intracellular ROS were determined by oxidation of dihydrorhodamine-123 (DHR-123) to rhodamine by spectrofluorescence. This probe measures levels of intermediates such as peroxy nitrite, H₂O₂, and OH[•] [34]. Briefly, MG-63 cells were incubated at 37 °C with $\text{SiO}_2@\text{ZrO}_2^{\text{cryst}}$ or $\text{SiO}_2@\text{ZrO}_2^{\text{am}}$. After 24 h, cells were incubated with 10 mM DHR-123. After 1 h, cells were scraped into 1 mL 0.1% Triton-X 100. The cell extracts were then analyzed for the oxidized product rhodamine by measuring fluorescence (excitation, 495 nm; emission, 532 nm), using a Perkin-Elmer LS-50B luminescence spectrometer (Beaconsfield, England) equipped with a pulsed xenon lamp (half peak height <10 µs, 60 Hz), an R928 photomultiplier tube and a computer (FL Winlab software). Results were corrected for protein content, measured with the Pierce™ BCA Protein Assay Kit.

2.2.8. Fluorometric determination of cellular GSH/GSSG ratio

GSH and GSSG levels were determined in cultured cells as follows. Confluent cell monolayers were incubated with $\text{SiO}_2@\text{ZrO}_2^{\text{cryst}}$ or $\text{SiO}_2@\text{ZrO}_2^{\text{am}}$ at 37 °C for 24 h. Monolayers were washed with PBS and harvested by incubation with 250 µL Triton 0.1% for 30 min. For GSH determination, aliquots (100 µL) were mixed with ice-cold phosphate buffer (Na₂HPO₄ 0.1 M; EDTA 5 mM; 1.8 mL) and 100 µL o-phthaldialdehyde (0.1% in methanol) as described by Hissin and Hilf [35]. For the determination of GSSG, aliquots (100 µL) were mixed with NaOH (0.1 M, 1.8 mL) and o-phthaldialdehyde as before. To avoid GSH oxidation, the cellular extracts for GSSG determination were incubated with 0.04 M N-ethylmaleimide. Fluorescence emission (420 nm; excitation, 350 nm) was determined. The GSH/GSSG ratio, which is a marker of cellular redox status, was calculated as % basal for all experimental conditions.

2.2.9. Uptake and subcellular localization by TEM

After treatment with 50 µg/mL $\text{SiO}_2@\text{ZrO}_2^{\text{cryst}}$ or $\text{SiO}_2@\text{ZrO}_2^{\text{am}}$, MG-63 cells were fixed in 2% glutaraldehyde for 1 h at 4 °C. Later, cells were treated with 2% OsO₄ in sodium cacodylate and embedded in epoxy resin, Epon (Serva, Heidelberg, Germany). Ultrathin sections (60 nm) were obtained with ultramicrotome (Supernova

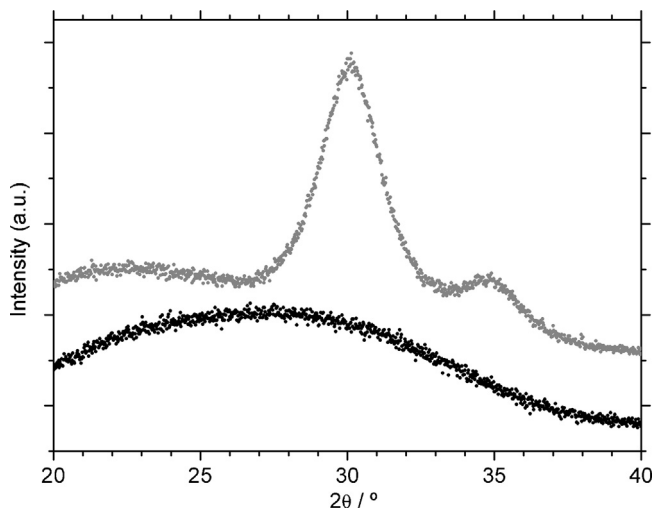


Fig. 1. X-ray results obtained before (bottom) and after (top) thermal treatment at 900 °C.

Reichert-J). These sections were stained with uranyl acetate solution in acetic acid and plumbic citrate. TEM analyses of ultrathin sections allowed determination of the agglomeration of the particles and their distribution within the cells, placing the ultrathin sections on 150 mesh grids and examining with a TEM microscope (JEOL JEM 1200 EX II).

2.2.10. Statistical analysis

Results are expressed as the mean of three independent experiments and plotted as mean \pm standard error of the mean (SEM). The total number of repeats (n) is specified in the legends of the figures. Statistical analysis of the data was carried out by ANOVA, followed by the Fisher' Least Significant Difference (LSD) procedure to discriminate among the means. The statistical analyses were performed using STATGRAPHICS Centurion XVI.I. In the comet assay, Mann-Whitney Rank Sum Test was carried out to compare treated cells group against the control group and against each other.

3. Results

3.1. Physicochemical characterization of the materials

Confirmation of the crystallization of the ZrO₂ shell after thermal treatment was performed by XRD. The X-ray diffractogram of calcined materials (Fig. 1) showed one main broad reflex centered at about 30° 2θ and a second reflex with lower intensity centered at about 35° 2θ, which was assigned to tetragonal zirconia. Moreover, a broad signal starting below 20° 2θ and extending almost up to 40° 2θ was observed, which was attributed to non-crystalline

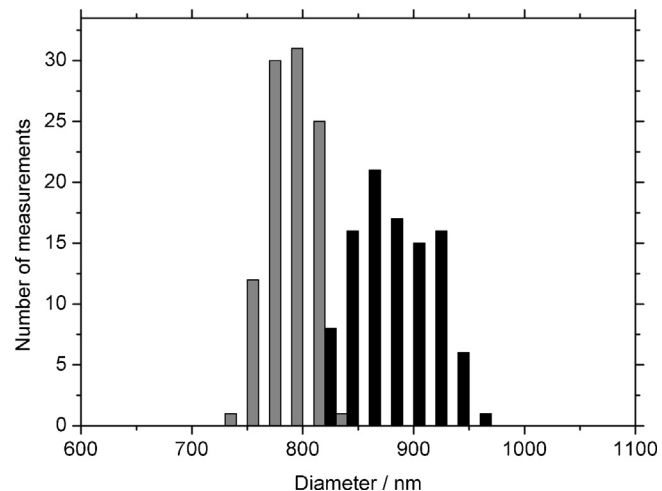


Fig. 3. Size distribution of SiO₂@ZrO₂^{cryst} and SiO₂@ZrO₂^{am}; the difference between both populations of particle diameters is statistically significant ($\alpha = 0.05$, One Way ANOVA).

SiO₂. Before the thermal treatment, diffractograms showed only the signal attributed to the non-crystalline solid (Fig. 1).

Core@shell particles were spherical, as determined by scanning electron microscopy (Fig. 2). Particles with non-crystalline shells had a mean diameter of 891 \pm 34 nm, while particles with crystalline shell had a mean diameter of 782 \pm 19 nm. Fig. 3 shows the size distribution of SiO₂@ZrO₂^{cryst} and SiO₂@ZrO₂^{am}; the difference between both populations of particle diameters is statistically significant ($\alpha = 0.05$, one-way ANOVA).

3.2. Effect of SiO₂@ZrO₂^{cryst} or SiO₂@ZrO₂^{am} on cell viability

The cytotoxicity of SiO₂@ZrO₂^{cryst} or SiO₂@ZrO₂^{am} was assayed in 24-h exposed MG-63 cells by measuring the ability to process MTT and by quantifying the total amount of cellular protein. Figs. 4 and 5 show the relationship between cell viability (as percentage absorbance of control value) and particle concentration. Alteration in cell energy metabolism can be monitored by measuring loss of the ability of mitochondria to reduce MTT to an insoluble violet product (formazan), and is related to cell viability. Exposing MG-63 cells to dispersions of either SiO₂@ZrO₂^{cryst} or SiO₂@ZrO₂^{am} at different concentrations (5–100 μ g/mL) showed that only SiO₂@ZrO₂^{cryst} induced a significant decrease in the ability of the cells to form the insoluble violet product, at 100 μ g/mL (Fig. 4, $p < 0.001$). Likewise, SiO₂@ZrO₂^{cryst} caused a significant decrease of the total protein content only at the higher tested concentration (Fig. 5, $p < 0.05$).

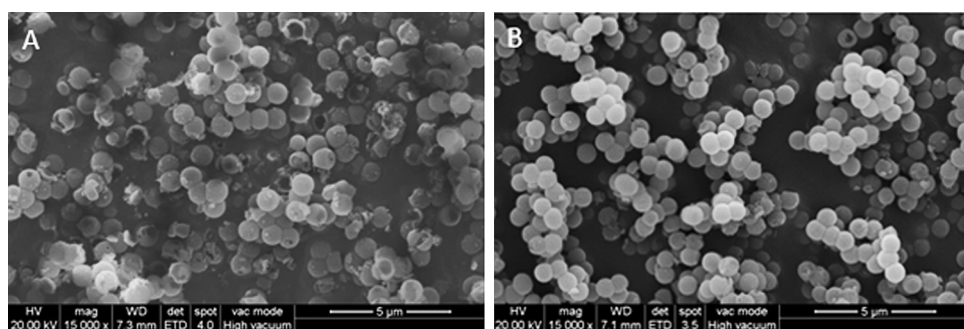


Fig. 2. SEM image of (A) SiO₂@ZrO₂^{am} and (B) SiO₂@ZrO₂^{cryst}.

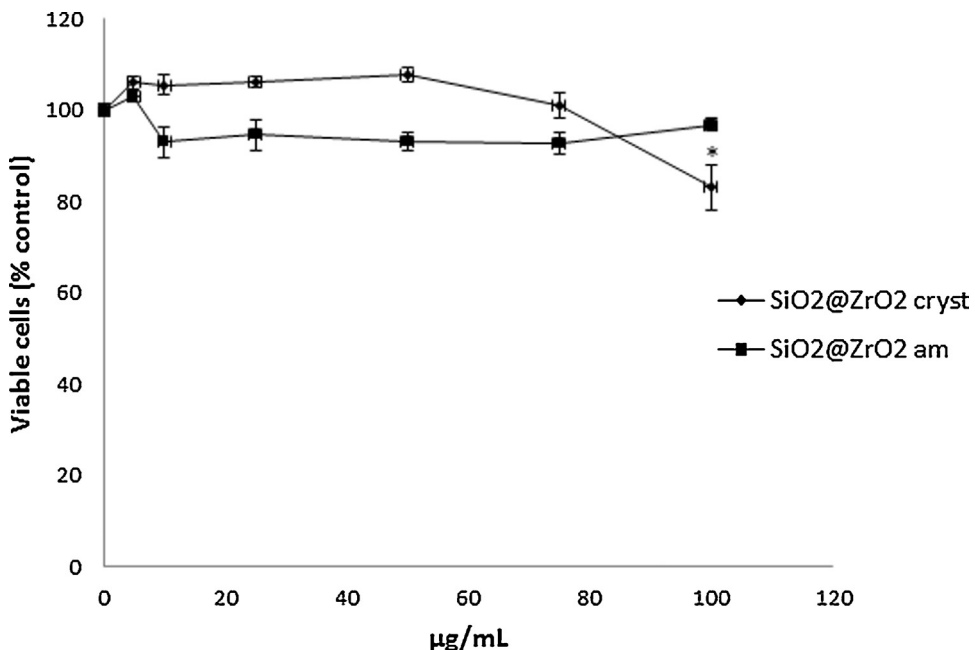


Fig. 4. MTT assay in MG-63 cells. After incubation with SiO₂@ZrO₂^{cryst} or SiO₂@ZrO₂^{am}, mitochondrial activity was determined by the conversion of the tetrazolium salt to a colored formazan by mitochondrial dehydrogenases. Color development was measured at 570 nm after cell lysis in DMSO. Results are expressed as % basal and represent the mean \pm SEM (standard error of the mean) ($n=24$), * significant differences versus control, $p < 0.001$.

3.3. Genotoxicity studies

We examined how SiO₂@ZrO₂^{cryst} and SiO₂@ZrO₂^{am} induced genotoxicity by looking at the increase of MN frequency and the induction of DNA damage by the comet assay. MN induction in binucleated cells was observed after exposure to either SiO₂@ZrO₂^{cryst} or SiO₂@ZrO₂^{am} for 24 h (Fig. 6). A concentration-related induction of MN was observed at concentrations above 25 μg/mL SiO₂@ZrO₂^{cryst}. On the other hand, the increase in MN frequency was only statistically significant at 50 μg/mL

SiO₂@ZrO₂^{am} ($p < 0.05$). The increased frequencies were even higher than for the bleomycin (BLM)-treated cells used as positive control.

The Single Cell Gel Electrophoresis (SCGE) or comet assay detects single- and double-strand DNA breaks. Under alkaline conditions, additional DNA damages are detected, such as abasic sites. As is shown in Fig. 7, SiO₂@ZrO₂^{cryst} and SiO₂@ZrO₂^{am} produced a significant genotoxic effect in MG-63 cells from 5 and 10 μg/mL ($p < 0.05$), respectively. Moreover, the genotoxicity increases with concentration, for both types of particles. At

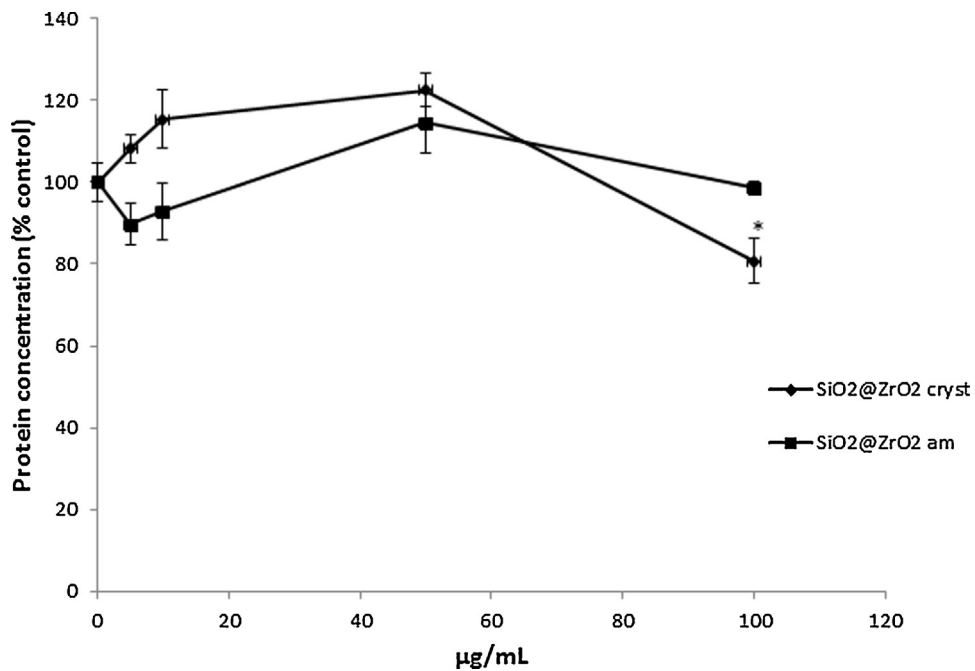


Fig. 5. Measurement of total protein content in MG-63 cells. After incubation with SiO₂@ZrO₂^{cryst} or SiO₂@ZrO₂^{am}, total protein content was determined by the BCA Protein Assay. Color development was measured at 540 nm. Results are expressed as % basal and represent the mean \pm SEM ($n=15$), * significant differences versus control, $p < 0.05$.

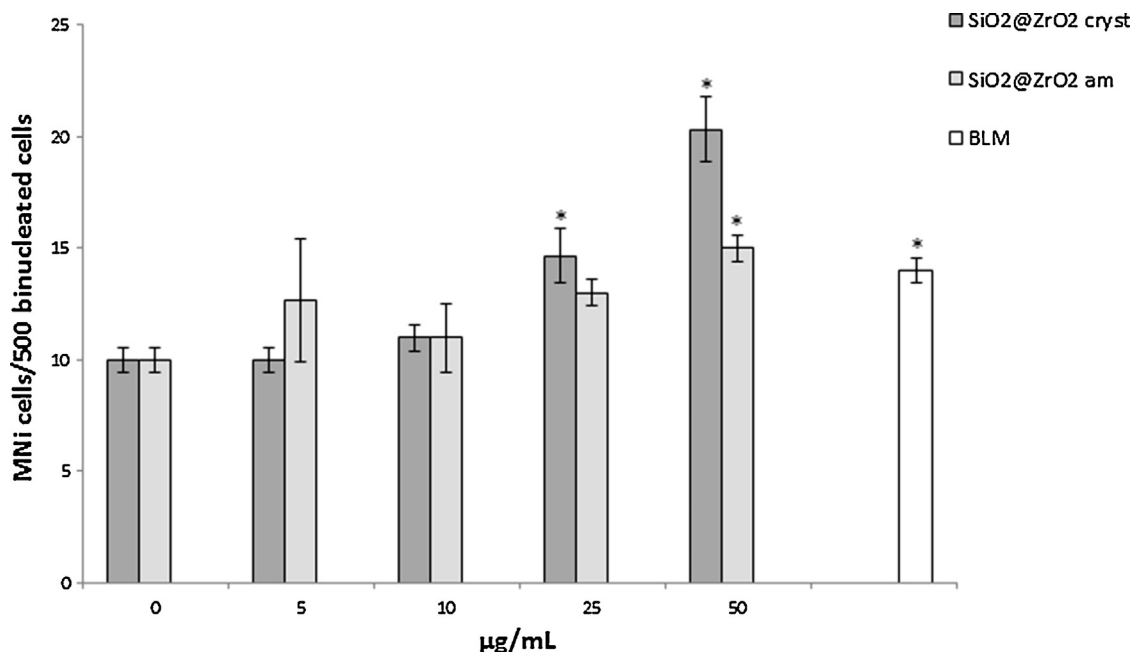


Fig. 6. Genotoxicity of SiO₂@ZrO₂ particles in MG-63 cells. Micronuclei induction in MG-63 cells after 24 h exposure to SiO₂@ZrO₂^{cryst} or SiO₂@ZrO₂^{am}. Results represent the mean \pm SEM ($n = 3$), * significant differences versus control, $p < 0.05$. BLM stands for Bleomycin used as a positive control.

50 µg/mL SiO₂@ZrO₂^{cryst}, there is a decline in the effect on the tail moment; however, the difference with the effect at the lower concentration (10 µg/mL) was not statistically significant. Altogether, these results suggest that crystalline zirconia-coated particles induced genotoxic effects at lower concentrations than the amorphous analogue.

3.4. Mechanism of action

For a better understanding of the possible mechanism involved in the cyto- and genotoxicity of zirconia-coated colloidal silica

spheres in MG-63 cells, we evaluated the effect on oxidative stress through the measurement of ROS level by the oxidation of the probe DHR-123 and the determination of the ratio of the redox couple GSH/GSSG. DHR-123 is a mitochondria-associated probe that is oxidized to rhodamine123, which can be detected by fluorescence. Only incubation of MG-63 osteosarcoma cells with SiO₂@ZrO₂^{cryst} caused an increase in induction of ROS, at the highest concentration tested (100 µg/mL), Fig. 8. At the highest concentration, SiO₂@ZrO₂^{cryst} caused 40% ROS increase over the basal level. However, SiO₂@ZrO₂^{am} did not change the ROS level, compared to control values.

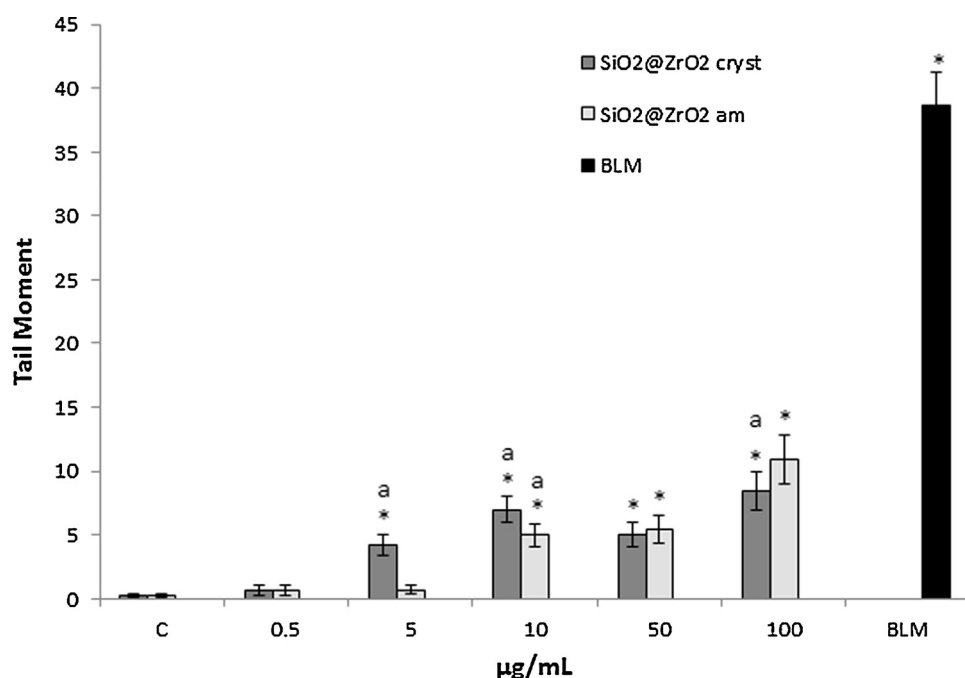


Fig. 7. Genotoxicity of SiO₂@ZrO₂ particles in MG-63 cells. Induction of DNA damage determined by SCGE (Comet assay) and evaluated by the Tail Moment. After incubation with SiO₂@ZrO₂^{cryst} or SiO₂@ZrO₂^{am} for 24 h, cells were lysed and DNA fragments were processed by electrophoresis. After that, the nuclei were stained and analyzed. Results represent the mean \pm SEM ($n = 150$), * significant differences versus control, ^a significant differences with the previous concentration, $p < 0.05$. BLM stands for Bleomycin used as a positive control.

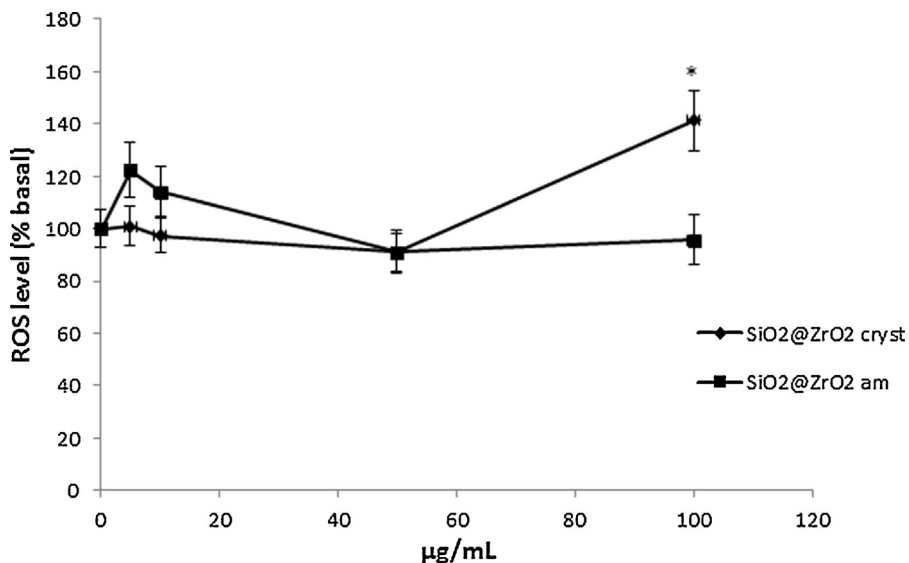


Fig. 8. Induction of ROS by SiO₂@ZrO₂ particles in MG-63 cell line. Cells were incubated with growing concentrations of SiO₂@ZrO₂^{cryst} or SiO₂@ZrO₂^{am} at 37 °C for 24 h. ROS production in the cells was evaluated through the oxidation of DHR-123 to Rhodamine123. Results are expressed as % basal and represent the mean ± SEM ($n=14$), *significant differences versus control, $p < 0.01$.

To get a broader knowledge on the factors involved in the cellular redox status, the GSH/GSSG ratio was also investigated. An increase in ROS levels may cause a reduction in GSH levels and/or an accumulation of GSSG inside the cells. Both SiO₂@ZrO₂^{cryst} and SiO₂@ZrO₂^{am} induced a decrease in the GSH/GSSG ratio in MG-63 cells in a concentration-dependent manner above 50 μg/mL ($p < 0.001$); Fig. 9.

3.5. Uptake and subcellular localization

SiO₂@ZrO₂ particles crossed the cell membrane. MG-63 cells treated with either SiO₂@ZrO₂^{cryst} or SiO₂@ZrO₂^{am} (50 μg/mL) for 24 h showed particles inside the cells (Fig. 10) included in intracellular vesicles into the cytoplasm. Interestingly, particles within the

cells were found exclusively in the cytoplasm and not inside the nucleus.

4. Discussion

The development of novel nanoparticles is currently undergoing a dramatic expansion. However, the potential toxicities of these new materials must be understood. Indeed, a detailed assessment of the factors that influence the biocompatibility and/or toxicity of nanoparticles is crucial for the safe and sustainable development of the emerging nanotechnologies [36,37]. Particularly, core@shell structures interest researchers in the field of biomedical engineering, since they have improved properties compared to alternatives [1].

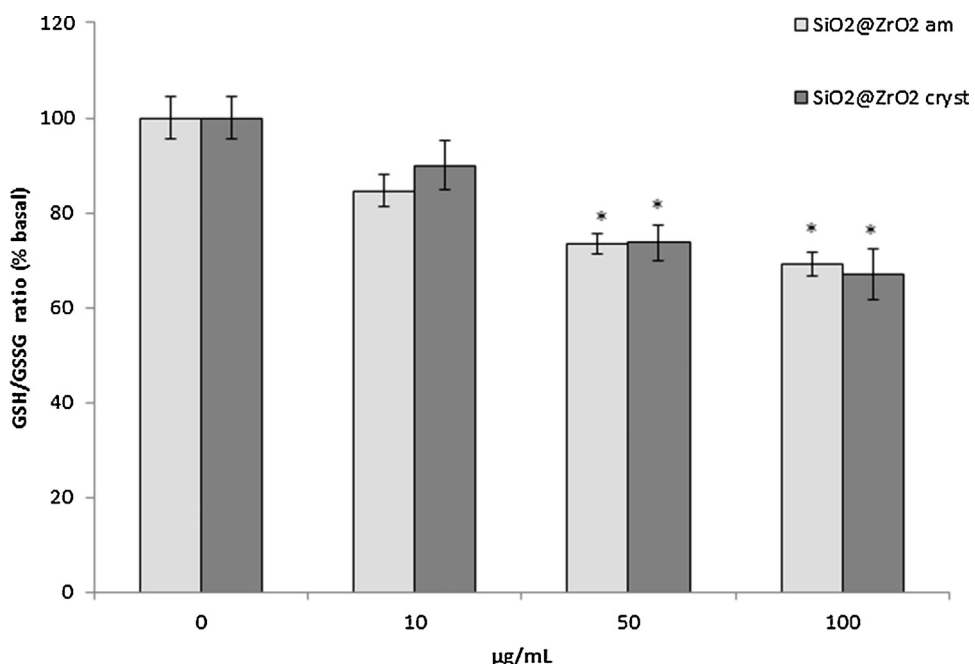


Fig. 9. Alteration of GSH/GSSG ratio by SiO₂@ZrO₂ particles in MG-63 cells. Results are expressed as % basal and represent the mean ± SEM ($n=9$), *significant differences versus control, $p < 0.001$.

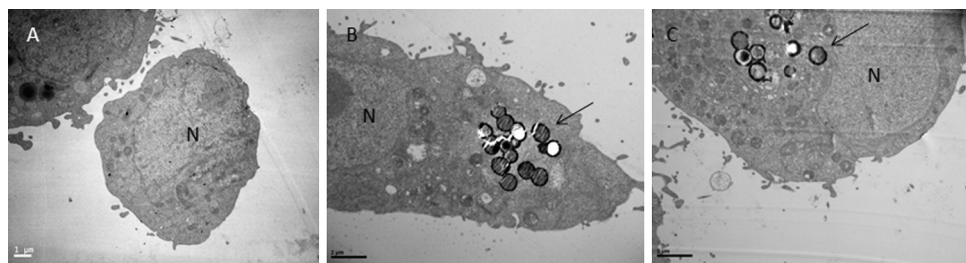


Fig. 10. Transmission electron photographs of MG-63 cells treated during 24 h with (B) $\text{SiO}_2@\text{TiO}_2^{\text{cryst}}$ 50 $\mu\text{g}/\text{mL}$; (C) $\text{SiO}_2@\text{TiO}_2^{\text{am}}$ 50 $\mu\text{g}/\text{mL}$. (A) Negative control. Intracellular phagocytosed material can be observed (black arrows) within vesicles. N: nucleus.

In the present study, cyto- and genotoxicity of colloidal core@shell particles with silica core coated with crystalline or amorphous zirconia were evaluated *in vitro* in human osteosarcoma MG-63 cells, and underlying mechanisms of action were tested.

4.1. Evaluation of the cytotoxic effects of zirconia-coated silica spheres

Cytotoxicity of $\text{SiO}_2@\text{ZrO}_2$ particles was evaluated by measurement of total protein content and by the MTT assay. A slight but statistically significant deleterious effect on viability of MG-63 cells was observed only after exposure with the slightly larger particles ($\text{SiO}_2@\text{ZrO}_2^{\text{cryst}}$) at the higher concentration tested in both assays, and was less than 20%. Higher concentrations were not examined because, at those concentrations, cells were covered by the particles, making microscopic observation difficult.

These findings agree with a previous observation where nano and bulk ZrO_2 particles did not alter microbial susceptibility [38]. Cytotoxicity induced by ceramic particles was studied in mammalian cells *in vitro*: ZrO_2 particles did not give rise to any significant difference up to 2500 particles per cell, and mortality remained very low (less than 10%) in J774 mouse macrophages [39].

Several reports point out a difference in toxicological behavior, depending on particle size. We have previously reported that spherical particles with an amorphous core of silica and a crystalline shell of titanium oxide nanocrystals ($\text{SiO}_2@\text{TiO}_2$) induced less decrease in cell viability in comparison to TiO_2 nanoparticles in UMR106 cells [40]. Moreover, it has been reported that micrometer-sized TiO_2 did not alter cell proliferation [41]; however, nanoparticles of the same chemical composition produced a decrease in cell viability in different cancer cell lines as well as cultured human cells [42–44]. On the contrary, cell viability studied in 3T3 mouse fibroblasts indicated that nano ZrO_2 and TiO_2 were less toxic than microparticles up to 200 $\mu\text{g}/\text{mL}$ [45].

Cytotoxicity of particles might be lessened by increasing the size or by the presence of the shell itself. Cell viability of core@shell materials has been evaluated *in vitro* in different systems. A recent study conducted to assess the biocompatibility of $\text{Fe}_3\text{O}_4@\text{Au}$ particles showed no cytotoxicity for this material on mouse fibroblast cell line [46]. Another report showed that $\text{ZnO}@\text{TiO}_2$ particles were less toxic than ZnO nanoparticles towards human epithelia cells [47]. Moreover, uptake and toxicity studies with $\text{Ru}@\text{SiO}_2$ nanoparticles in early life stages of Zebra fish embryos *in vivo* showed that they mainly accumulate on the chorion of embryos and exhibit no overt embryotoxicity [48].

4.2. Genotoxic effects of zirconia-coated silica spheres

As DNA damage plays an important role in carcinogenesis, we investigated whether core@shell spheres were able to induce genetic damage in human osteosarcoma cells *in vitro*. One indicator

of genotoxicity is increased MN frequency. We observed increased MN frequency in binucleated MG-63 cells exposed to $\text{SiO}_2@\text{ZrO}_2$ particles. However, $\text{SiO}_2@\text{ZrO}_2^{\text{cryst}}$ induced a stronger and statistically different response in comparison to $\text{SiO}_2@\text{ZrO}_2^{\text{am}}$. Moreover, the genotoxic effect started at lower concentration.

Another indicator of genotoxicity is the DNA damage observed by the induction of 'comets'. Under alkaline conditions, the comet assay detects single- and double-strand DNA breaks as well as sites where excisions and repairs have occurred [49]. We evaluated the tail moment parameter which is defined as the Tail Length \times DNA amount in the tail. DNA amount is determined through the intensity of fluorescence. The distance of DNA migration is used to measure the extent of DNA damage. However, if DNA damage is relatively high, the tail increases in fluorescent staining intensity but not in length. For these reasons, it is useful to use the Tail Moment as a genotoxic endpoint [50]. In this assay, we demonstrated that $\text{SiO}_2@\text{ZrO}_2^{\text{cryst}}$ induced a significant genotoxic effect in MG-63 cells, which began at a lower concentration than $\text{SiO}_2@\text{ZrO}_2^{\text{am}}$. Overall, these results suggest that both particles induced DNA breaks in MG-63 cells, leading to a positive result in the comet assay and MN induction. However the genotoxic effect of the crystalline form is detected at lower concentrations.

Previous studies have demonstrated the genotoxicity of hydroxylapatite/ ZrO_2 composite particles, studied by the MN assay. The genotoxic effect increased with a higher proportion of ZrO_2 and with the increase in the concentration of the composite [51]. On the contrary, it has been reported that there was no significant difference in MN formation rates when L929 cells were exposed to $\text{Fe}_3\text{O}_4@\text{Au}$ composite magnetic nanoparticles [46].

4.3. Particle size and crystalline structure-dependence toxicity

In the current study, $\text{SiO}_2@\text{ZrO}_2^{\text{cryst}}$ and $\text{SiO}_2@\text{ZrO}_2^{\text{am}}$ particles present equivalent chemical composition. However, only the former exhibits crystalline structure at the shell. This could be one explanation for the genotoxicity differences. In the last decade, toxicological studies have demonstrated that adverse effects may be dependent on the surface area of nanoparticles [52–56]. Particularly, it has been demonstrated that cytotoxicity and cellular uptake of silica@polymer nanospheres in mouse macrophage RAW 264.7 and rat pheochromocytoma PC-12 cells *in vitro* depend on surface composition [57]. Moreover, toxicity of a material may also depend on its crystalline form, as demonstrated for rutile and anatase titanium dioxide, which have the same chemical composition but different crystalline structure, and hence different chemical and physical properties [52]. Another explanation for the differences found in the cytotoxicity and genotoxicity tests might be particle size. Particles with non-crystalline shells had a mean diameter of 891 ± 34 nm, while particles with crystalline shell had a mean diameter of 782 ± 19 nm. This difference, although small, could cause diverse results in the toxicological studies. Previously, it has been demonstrated that particle size is a very important

physico-chemical characteristic in determining the adverse health effects [58,59].

4.4. Mechanism of action

Given that nanoparticles induce ROS-mediated genotoxicity in mammalian cells [60–63], we have investigated the putative cell death mechanisms triggered by the particles on osteoblast-like cells through the determination of the oxidative stress by means of ROS production and the GSH/GSSG ratio. Particle toxicity has been previously associated with capacity to induce formation of ROS, probably by interacting with mitochondrial redox centers [64–66]. GSH is one of the major reducing agents in mammalian cells. This thiol acts by sequestering free radicals and regulating the redox status by means of the couple GSH/GSSG [67]. A sustained increase in ROS levels may cause an accumulation of GSSG inside the cells. Because of this, the determination of GSH/GSSG ratio is relevant to the investigation of oxidative stress [68].

Our findings showed that only $\text{SiO}_2@\text{ZrO}_2^{\text{cryst}}$ induced an increase in ROS levels in MG-63 cells at the highest concentration assayed, which may explain its toxic action associated with mitochondrial injury (MTT assay) or with the decrease of the total protein content. $\text{SiO}_2@\text{ZrO}_2^{\text{am}}$ did not produce an increase in ROS levels in the cells. This effect agrees with the results in the cell viability assays, which showed no statistically significant modification. Moreover, both types of particles induced a decrease in the GSH/GSSG ratio in MG-63 human osteosarcoma cell line reaching about 65% at the higher doses (50 and 100 $\mu\text{g/mL}$). Overall, it can be assumed that in $\text{SiO}_2@\text{ZrO}_2^{\text{cryst}}$ -treated cells, the free radicals decrease the concentration of important cellular compounds and cause weakness of the antioxidant system, making the cells more vulnerable to oxidative damage. These results suggest that the depletion of GSH concentration would mediate the cytotoxic action of the crystalline zirconia-coated particles. On the other hand, the relationship between ROS levels and GSH/GSSG ratio in $\text{SiO}_2@\text{ZrO}_2^{\text{am}}$ -treated cells is very intricate since no evident correlation could be established. In fact, these particles maintained ROS levels at control values determined by DHR-123 method. Nevertheless, they caused a decrease of GSH/GSSG ratio. A mechanism involved in the deleterious action of the particles on these thiol-containing molecules may be related to the effect of other free radicals that cannot be detected by DHR-123 probe such as superoxide radical anion [69,70].

With regard to particle genotoxicity, the increase in ROS levels measured by the oxidation of DHR-123 and the decrease of the GSH/GSSG ratio could explain the genotoxic damage at the higher concentrations ($>50 \mu\text{g/mL}$). However, at lower concentrations, other mechanisms of genotoxicity could take place [71]. The elicitation of genetic damage in the absence of inflammation might be caused by an indirect mechanism that results from the enhanced production of ROS by cellular constituents including mitochondria or by a direct mechanism involving the interaction of particles with DNA, that is, a direct physical interaction upon entry of particles into the nucleus [72]. However, genotoxicity induced by particles has been described in the absence of particles within the nucleus. This effect could be the result of the release of low-molecular-weight substances which can diffuse into the nucleus (such as transition metal ions), or oxidizing species generated near the surfaces of the particles (such as 4-hydroxy-2-nonenal or peroxynitrite) [71].

Physical mechanisms which induce deleterious actions depend on the size and the surface of the particle [73], and include disruption of lipid membranes, formation of holes and/or thinned regions [74], unfolding of proteins [75], and inactivation of specific DNA repair proteins due to the process of adsorption, which often results in conformational changes of intracellular proteins and exposure

of amino acid residues that are normally buried in the core of the native protein, as was demonstrated for metallic nanoparticles [76].

4.5. TEM observations

In an attempt to gain deeper insight in the mechanism involved in the toxicity of colloidal silica spheres coated with crystalline or amorphous zirconia on human osteosarcoma cells, we studied the uptake and subcellular localization of the particles by TEM. After 24 h exposure, colloidal particles crossed the cell membrane and formed intracellular vesicles; however, they remained outside the nucleus. These findings agree with the previously reported intracellular localization of colloidal silica spheres coated with crystalline titanium dioxide particles in murine osteosarcoma cells [40]. Internalization of particles exclusively in the cytoplasm has also been observed with other particles and different cells [77,78]. Internalization of particles in MG-63 cells may proceed via pinocytosis, which is a fluid-phase endocytosis mechanism which occurs when particles bind to cell membranes and lead to the formation of vesicles [79,80]. This phenomenon might explain the particle internalization arranged in perinuclear fashion observed in the present investigation.

5. Conclusions

Colloidal silica spheres coated with crystalline or amorphous zirconia were found inside the cells, forming vesicles; however, none of them entered the nucleus. $\text{SiO}_2@\text{ZrO}_2^{\text{cryst}}$ reduced cell viability at 100 $\mu\text{g/mL}$, associated with an increase of ROS formation and depletion of thiol-reducing agents. These effects could be related to DNA damage detected by the comet and MN assays. $\text{SiO}_2@\text{ZrO}_2^{\text{am}}$ caused neither cell viability reduction nor increase of ROS levels at the range of concentrations studied (up to 100 $\mu\text{g/mL}$). However, these particles produced DNA damage according to the comet and MN assays. Overall, our results suggest that crystallization of the shell of the amorphous ZrO_2 , generated by a thermal treatment into nanocrystals, increased the cyto- and genotoxicity, indicating particle size- and crystalline structure-dependent toxicity.

Conflict of interest

The authors declare that there are no conflicts of interest.

Acknowledgments

This study was partially supported by ANPCyT (PICT 2010-0981), by Comisión de Investigaciones Científicas de la Provincia de Buenos Aires (fellowship for undergraduate students) and by the Centro de Tecnología de Recursos Minerales y Cerámica (CETMIC). Dr. Ana Laura Di Virgilio and Dr. Pablo M. Arnal are members of CONICET Argentina.

References

- [1] N. Soundarya, Y. Zhang, Use of core/shell structured nanoparticles for biomedical applications, *Recent Patents Biomed. Eng.* 1 (2008) 34–42.
- [2] K.S. Oh, S.K. Han, Y.W. Choi, J.H. Lee, J.Y. Lee, S.H. Yuk, Hydrogen-bonded polymer gel and its application as a temperature-sensitive drug delivery system, *Biomaterials* 25 (2004) 2393–2398.
- [3] A.J.P. Van Zyl, R.D. Sanderson, D. De Wet-Roos, B. Klumperman, Core/shell particles containing liquid cores: morphology prediction, synthesis, and characterization, *Macromolecules* 36 (2003) 8621–8629.
- [4] J.I. Arias, M. López-Viota, M.A. Ruiz, J. López-Viota, A.V. Delgado, Development of carbonyl iron/ethylcellulose core/shell nanoparticles for biomedical applications, *Int. J. Pharm.* 339 (2007) 237–245.
- [5] P. Botella, A. Corma, M.T. Navarro, Single gold nanoparticles encapsulated in monodispersed regular spheres of mesostructured silica produced by pseudomorphic transformation, *Chem. Mater.* 19 (2007) 1979–1983.

- [6] S.J. Hwang, J.-h. Lee, Mechanochemical synthesis of Cu-Al₂O₃ nanocomposites, *Mater. Sci. Eng. A* 405 (2005) 140–146.
- [7] G.H. Du, Z.L. Liu, X. Xia, Q. Chu, S.M. Zhang, Characterization and application of Fe₃O₄/SiO₂ nanocomposites, *J. Sol-Gel Sci. Technol.* 39 (2006) 285–291.
- [8] W. Fu, H. Yang, Q. Yu, J. Xu, X. Pang, G. Zou, Preparation and magnetic properties of SrFe12O19/SiO₂ nanocomposites with core–shell structure, *Mater. Lett.* 61 (2007) 2187–2190.
- [9] A. Nel, T. Xia, L. Mädler, N. Li, Toxic potential of materials at the nanolevel, *Science* 311 (2006) 622–627.
- [10] C.M. Sayes, K.L. Reed, D.B. Warheit, Assessing toxicity of fine and nanoparticles: comparing in vitro measurements to in vivo pulmonary toxicity profiles, *Toxicol. Sci.* 97 (2007) 163–180.
- [11] V. Stone, I.A. Kinloch, M. Clift, T.F. Fernandes, A.T. Ford, N. Christofi, A. Griffiths, K. Donaldson, Nanoparticle toxicology and ecotoxicology. The role of oxidative stress, in: Y. Zhao, H.S. Nalwa (Eds.), *Nanotoxicology – Interactions of Nanomaterials with Biological Systems*, American Scientific Publishers, 2006.
- [12] T. Xia, M. Kovochich, J. Brant, M. Hotze, J. Sempf, T. Oberley, C. Sioutas, J.I. Yeh, M.R. Wiesner, A.E. Nel, Comparison of the abilities of ambient and manufactured nanoparticles to induce cellular toxicity according to an oxidative stress paradigm, *Nano Lett.* 6 (2006) 1794–1807.
- [13] A. Banasik, A. Lankoff, A. Piskulak, K. Adamowska, H. Lisowska, A. Wojcik, Aluminum-induced micronuclei and apoptosis in human peripheral-blood lymphocytes treated during different phases of the cell cycle, *Environ. Toxicol.* 20 (2005) 402–406.
- [14] P.J. Lu, I.C. Ho, T.C. Lee, Induction of sister chromatid exchanges and micronuclei by titanium dioxide in Chinese hamster ovary-K1 cells, *Mutat. Res. Gen. Toxicol. Environ. Mutagen.* 414 (1998) 15–20.
- [15] A. Lankoff, A. Banasik, A. Duma, E. Ochniak, H. Lisowska, T. Kuszewski, S. Góźdż, A. Wojcik, A comet assay study reveals that aluminium induces DNA damage and inhibits the repair of radiation-induced lesions in human peripheral blood lymphocytes, *Toxicol. Lett.* 161 (2006) 27–36.
- [16] P.D.L. Lima, D.S. Leite, M.C. Vasconcellos, B.C. Cavalcanti, R.A. Santos, L.V. Costa-Lotufo, C. Pessoa, M.O. Moraes, R.R. Burbano, Genotoxic effects of aluminum chloride in cultured human lymphocytes treated in different phases of cell cycle, *Food Chem. Toxicol.* 45 (2007) 1154–1159.
- [17] E. Theogaraj, S. Riley, L. Hughes, M. Maier, D. Kirkland, An investigation of the photo-clastogenic potential of ultrafine titanium dioxide particles, *Mutat. Res. Gen. Toxicol. Environ. Mutagen.* 634 (2007) 205–219.
- [18] D.B. Warheit, R.A. Hoke, C. Finlay, E.M. Donner, K.L. Reed, C.M. Sayes, Development of a base set of toxicity tests using ultrafine TiO₂ particles as a component of nanoparticle risk management, *Toxicol. Lett.* 171 (2007) 99–110.
- [19] M.M. Rashad, H.M. Baioumi, Effect of thermal treatment on the crystal structure and morphology of zirconia nanopowders produced by three different routes, *J. Mater. Process. Technol.* 195 (2008) 178–185.
- [20] C.A. Maziero Volpatto, L.G.D. Altoé Garbelotto, M.R.C. Fredel, F. Bondioli, Application of zirconia in dentistry: biological mechanical and optical considerations, in: C. Sikalidis (Ed.), *Advances in Ceramics – Electric and Magnetic Ceramics, Bioceramics, Ceramics and Environment*, 2011.
- [21] M. Gahlert, T. Gudehus, S. Eichhorn, E. Steinhauser, H. Kniha, W. Erhardt, Biomechanical and histomorphometric comparison between zirconia implants with varying surface textures and a titanium implant in the maxilla of miniature pigs, *Clin. Oral Implants Res.* 18 (2007) 662–668.
- [22] M. Andreiotelli, H.J. Wenz, R.-J. Kohal, Are ceramic implants a viable alternative to titanium implants? A systematic literature review, *Clin. Oral Implants Res.* 20 (2009) 32–47.
- [23] Y. Ichikawa, Y. Akagawa, H. Nikai, H. Tsuru, Tissue compatibility and stability of a new zirconia ceramic in vivo, *J. Prosthet. Dent.* 68 (1992) 322–326.
- [24] T. Vaggopoulou, S. Koutayas, P. Koidis, J.R. Strub, Zirconia in dentistry: Part 1. Discovering the nature of an upcoming bioceramic, *Eur. J. Esthet. Dent.* 4 (2009) 130–151.
- [25] J. Chevalier, What future for zirconia as a biomaterial? *Biomaterials* 27 (2006) 535–543.
- [26] S. Lanone, F. Rogerieux, J. Geys, A. Dupont, E. Maillet-Marechal, J. Boczkowski, G. Lacroix, P. Hoet, Comparative toxicity of 24 manufactured nanoparticles in human alveolar epithelial and macrophage cell lines, *Part. Fibre Toxicol.* 6 (2009), <http://dx.doi.org/10.1186/1743-8977-6-14>.
- [27] L. Otero-Gonzalez, C. Garcia-Sauco, J.A. Field, R. Sierra-Alvarez, Toxicity of TiO₂, ZrO₂, Fe(0), Fe₂O₃, and Mn₂O₃ nanoparticles to the yeast, *Saccharomyces cerevisiae*, *Chemosphere* 93 (2013) 1201–1206.
- [28] L. Velzeboer, A.J. Hendriks, A.M. Ragas, D. Van de Meent, Aquatic ecotoxicity tests of some nanomaterials, *Environ. Toxicol. Chem.* 27 (2008) 1942–1947.
- [29] P.M. Arnal, C. Weidenthaler, F. Schuetz, Highly monodisperse zirconia-coated silica spheres and zirconia/silica hollow spheres with remarkable textural properties, *Chem. Mater.* 18 (2006) 2733–2739.
- [30] T. Mosmann, Rapid colorimetric assay for cellular growth and survival: application to proliferation and cytotoxicity assays, *J. Immunol. Methods* 65 (1983) 55–63.
- [31] H. Stopper, S.O. Müller, Micronuclei as a biological endpoint for genotoxicity: a mini review, *Toxicol. in Vitro* 11 (1997) 661–667.
- [32] M. Fenech, The in vitro micronucleus technique, *Mutat. Res.* 455 (2000) 81–95.
- [33] N.P. Singh, M.T. McCoy, R.R. Tice, E.L. Schneider, A simple technique for quantitation of low levels of DNA damage in individual cells, *Exp. Cell Res.* 175 (1988) 184–191.
- [34] J.A. Royal, H. Ischiropoulos, Evaluation of 2',7'-dichlorofluorescin and dihydrorhodamine 123 as fluorescent probes for intracellular H₂O₂ in cultured endothelial cells, *Arch. Biochem. Biophys.* 302 (1993) 348–355.
- [35] P.J. Hissin, R. Hilf, A fluorometric method for determination of oxidized and reduced glutathione in tissues, *Anal. Biochem.* 74 (1976) 214–226.
- [36] D. Warheit, C.M. Sayes, K.L. Reed, K.A. Swain, Health effects related to nanoparticle exposures: environmental, health and safety considerations for assessing hazards and risks, *Pharmacol. Ther.* 120 (2008) 35–42.
- [37] B. Fadeel, A.E. Garcia-Bennett, Better safe than sorry: understanding the toxicological properties of inorganic nanoparticles manufactured for biomedical applications, *Adv. Drug Deliv. Rev.* 62 (2010) 362–374.
- [38] G. Karunakaran, R. Suriyaprabha, P. Manivasakan, R. Yuvakkumar, V. Rajendran, N. Kannan, Impact of nano and bulk ZrO₂, TiO₂ particles on soil nutrient contents and PGPR, *J. Nanosci. Nanotechnol.* 13 (2013) 678–685.
- [39] I. Catelas, A. Petit, R. Marchand, D.J. Zukor, L.H. Yahia, O.L. Huk, Cyotoxicity and macrophage cytokine release induced by ceramic and polyethylene particles in vitro, *J. Bone Joint Surg. Br.* 81-B (1999) 516–521.
- [40] A.L. Di Virgilio, I. Maisuls, F. Kleitz, P.M. Arnal, A new synthesis pathway for colloidal silica spheres coated with crystalline TiO₂ and its comparative cytotoxic and genotoxic study with titanium oxide nanoparticles in rat osteosarcoma (UMR106) cells, *J. Colloid Interface Sci.* 394 (2013) 147–156.
- [41] J. Wu, J. Sun, Y. Xue, Involvement of JNK and P53 activation in G2/M cell cycle arrest and apoptosis induced by titanium dioxide nanoparticles in neuron cells, *Toxicol. Lett.* 199 (2010) 269–276.
- [42] P. Thevenot, J. Cho, D. Wavhal, R.B. Timmons, L. Tang, Surface chemistry influences cancer killing effect of TiO₂ nanoparticles, *Nanomedicine* 4 (2008) 226–236.
- [43] J.J. Wang, B.J.S. Sanderson, H. Wang, Cyto- and genotoxicity of ultrafine TiO₂ particles in cultured human lymphoblastoid cells, *Mutat. Res.* 628 (2007) 99–106.
- [44] M. Simon, P. Barberet, M.H. Delville, P. Moretto, H. Seznec, Titanium dioxide nanoparticles induced intracellular calcium homeostasis modification in primary human keratinocytes. Towards an in vitro explanation of titanium dioxide nanoparticles toxicity, *Nanotoxicology* 5 (2011) 125–139.
- [45] G. Karunakaran, R. Suriyaprabha, P. Manivasakan, R. Yuvakkumar, V. Rajendran, N. Kannan, Screening of in vitro cytotoxicity, antioxidant potential and bioactivity of nano- and micro-ZrO₂ and -TiO₂ particles, *Ecotoxicol. Environ. Safety* 93 (2013) 191–197.
- [46] Y. Li, J. Liu, Y. Zhong, J. Zhang, Z. Wang, L. Wang, Y. An, M. Lin, Z. Gao, D. Zhang, Biocompatibility of Fe₃O₄@Au composite magnetic nanoparticles in vitro and in vivo, *Int. J. Nanomed.* 6 (2011) 2805–2819.
- [47] I.L. Hsiao, Y.J. Huang, Titanium oxide shell coatings decrease the cytotoxicity of ZnO nanoparticles, *Chem. Res. Toxicol.* 24 (2011) 303–313.
- [48] K. Fent, C.J. Weisbrod, A. Wirth-Heller, U. Pieles, Assessment of uptake and toxicity of fluorescent silica nanoparticles in zebrafish (*Danio rerio*) early life stages, *Aquat. Toxicol.* 100 (2010) 218–228.
- [49] A.R. Collins, V.L. Dobson, M. Dušinská, G. Kennedy, R. Štětina, The comet assay: what can it really tell us? *Mutat. Res. Fund. Mol. Mech. Mutagen.* 375 (1997) 183–193.
- [50] W. Liao, M.A. McNutt, W.-G. Zhu, The comet assay: a sensitive method for detecting DNA damage in individual cells, *Methods* 48 (2009) 46–53.
- [51] R. Quan, Y. Tang, Z. Huang, J. Xu, X. Wu, D. Yang, Study on the Genotoxicity of HA/ZrO₂ Composite Particles in Vitro, *Mater. Sci. Eng. C. Mater. Biol. Appl.* 33 (2013) 1332–1338.
- [52] J.R. Gurr, A.S.S. Wang, C.H. Chen, K.Y. Jan, Ultrafine titanium dioxide particles in the absence of photoactivation can induce oxidative damage to human bronchial epithelial cells, *Toxicology* 213 (2005) 66–73.
- [53] G. Oberdörster, E. Oberdörster, J. Oberdörster, Nanotoxicology: An Emerging Discipline Evolving from Studies of Ultrafine Particles, *Environ Health Perspect.* 113 (2005) 823–839.
- [54] K. Donaldson, V. Stone, Current Hypotheses on the Mechanisms of Toxicity of Ultrafine Particles, *Ann. Ist Super Sanita* 39 (2003) 405–410.
- [55] M.R. Wilson, J.H. Lightbody, K. Donaldson, J. Sales, V. Stone, Interactions between ultrafine particles and transition metals in vivo and in vitro, *Toxicol. Appl. Pharmacol.* 184 (2002) 172–179.
- [56] G. Oberdoerster, J. Ferin, B.E. Lehner, Correlation between particle size, in vivo particle persistence, and lung injury, *Environ. Health Perspect.* 5 (1994) 173–179.
- [57] Y.S. Jeong, W.K. Oh, S. Kim, J. Jang, Cellular uptake, cytotoxicity, and ROS generation with silica/conducting polymer core/shell nanospheres, *Biomaterials* 32 (2011) 7217–7225.
- [58] G. Oberdörster, Toxicokinetics and effects of fibrous and nonfibrous particles, *Inhal. Toxicol.* 14 (2002) 29–56.
- [59] P.J.A. Borm, R.P.F. Schins, C. Albrecht, Inhaled particles and lung cancer, part B: paradigms and risk assessment, *Int. J. Cancer* 110 (2004) 3–14.
- [60] D. Walczyk, F.B. Bombelli, M.P. Monopoli, I. Lynch, K.A. Dawson, What the Cell Sees in Bionanoscience, *J. Am. Chem. Soc.* 132 (2010) 5761–5768.
- [61] S. Laurent, C. Burteau, C. Thirifays, U.O. Häfeli, M. Mahmoudi, Crucial ignored parameters on nanotoxicology: the importance of toxicity assay modifications and cell vision, *PLoS ONE* 7 (2012) e29997.
- [62] Q. Rahman, M. Lohani, E. Dopp, H. Pemsel, L. Jonas, D.G. Weiss, D. Schiffmann, Evidence that ultrafine titanium dioxide induces micronuclei and apoptosis in syrian hamster embryo fibroblasts, *Environ. Health Perspect.* 110 (2002) 797–800.
- [63] L.V. Akhal'tseva, N.E. Moshkov, F.I. Ingel, N.A. Iurtseva, V.V. Iurchenko, [Effect of titanium dioxide nano- and microparticles on the values of the micronucleus test using human blood lymphocytes in culture] 5 (2011) 61–63.

- [64] J. Wang, J. Ma, L. Dong, Y. Hou, X. Jia, X. Niu, Y. Fan, Effect of anatase TiO₂ nanoparticles on the growth of RSC-364 rat synovial cell, *J. Nanosci. Nanotechnol.* 13 (2013) 3874–3879.
- [65] C. Gunawan, A. Sirimanoonphan, W.Y. Teoh, C.P. Marquis, R. Amal, Submicron and nano formulations of titanium dioxide and zinc oxide stimulate unique cellular toxicological responses in the green microalga *Chlamydomonas reinhardtii*, *J. Hazard. Mater.* 260 (2013) 984–992.
- [66] B. Behl, I. Papageorgiou, C. Brown, R. Hall, J.L. Tipper, J. Fisher, E. Ingham, Biological effects of cobalt-chromium nanoparticles and ions on dural fibroblasts and dural epithelial cells, *Biomaterials* 34 (2013) 3547–3558.
- [67] D.P. Jones, J.L. Carlson, V.C. Mody, J. Cai, M.J. Lynn, P. Sternberg, Redox state of glutathione in human plasma, *Free Radic. Biol. Med.* 28 (2000) 625–635.
- [68] C. Hwang, A.J. Sinskey, H.F. Lodish, Oxidized redox state of glutathione in the endoplasmic reticulum, *Science* 257 (1992) 1496–1502.
- [69] K. Schuessel, C. Frey, C. Jourdan, U. Keil, C.C. Weber, F. Muller-Spahn, W.E. Muller, A. Eckert, Aging sensitizes toward ROS formation and lipid peroxidation in PS1M146L transgenic mice, *Free Radic. Biol. Med.* 40 (2006) 850–862.
- [70] Y. Qin, M. Lu, X. Gong, Dihydrorhodamine 123 is superior to 2,7-dichlorodihydrofluorescein diacetate and dihydorhodamine 6G in detecting intracellular hydrogen peroxide in tumor cells, *Cell Biol. Int.* 32 (2008) 224–228.
- [71] K. Donaldson, C.A. Poland, R.P.F. Schins, Possible genotoxic mechanisms of nanoparticles: criteria for improved test strategies, *Nanotoxicology* 4 (2010) 414–420.
- [72] L. Gonzalez, D. Lison, M. Kirsch-Volders, Genotoxicity of engineered nanomaterials: a critical review, *Nanotoxicology* 2 (2008) 252–273.
- [73] D. Walczyk, F.B. Bombelli, M.P. Monopoli, I. Lynch, K.A. Dawson, What the cell sees in bionanosciences, *J. Am. Chem. Soc.* 132 (2010) 5761–5768.
- [74] P.R. Leroueil, S.A. Berry, K. Duthie, G. Han, V.M. Rotello, D.Q. McNerny, J.R. Baker Jr., B.G. Orr, M.M.B. Holl, Wide varieties of cationic nanoparticles induce defects in supported lipid bilayers, *Nano Lett.* 8 (2008) 420–424.
- [75] P. Billsten, P.O. Freskgård, U. Carlsson, B.H. Jonsson, H. Elwing, Adsorption to silica nanoparticles of human carbonic anhydrase II and truncated forms induce a molten-globule-like structure, *FEBS Lett.* 402 (1997) 67–72.
- [76] I. Lynch, K.A. Dawson, S. Linse, Detecting cryptic epitopes created by nanoparticles, *Science's STKE: Signal Transduction Knowledge Environment* (2006).
- [77] A. Gojova, B. Guo, R.S. Kota, J.C. Rutledge, I.M. Kennedy, A.I. Barakat, Induction of inflammation in vascular endothelial cells by metal oxide nanoparticles: effect of particle composition, *Environ. Health Perspect.* 115 (2007) 403–409.
- [78] A. Simon-Deckers, B. Gouget, M. Mayne-L'Hermitte, N. Herlin-Boime, C. Reynaud, M. Carrière, In vitro investigation of oxide nanoparticle and carbon nanotube toxicity and intracellular accumulation in A549 human pneumocytes, *Toxicology* 253 (2008) 137–146.
- [79] R. Shukla, V. Bansal, M. Chaudhary, A. Basu, R.R. Bhonde, M. Sastry, Biocompatibility of gold nanoparticles and their endocytotic fate inside the cellular compartment: a microscopic overview, *Langmuir* 21 (2005) 10644–10654.
- [80] H. Suzuki, T. Toyooka, Y. Ibuki, Simple and easy method to evaluate uptake potential of nanoparticles in mammalian cells using a flow cytometric light scatter analysis, *Environ. Sci. Technol.* 41 (2007) 3018–3024.